EPR identification of the negatively charged vacancy in diamond

J. Isoya
University of Library and Information Science, 1-2 Kasuga, Tsukuba-City, Ibaraki 305, Japan

H. Kanda, Y. Uchida, and S. C. Lawson
National Institute for Research in Inorganic Materials, 1-1 Namiki, Tsukuba-City, Ibaraki 305, Japan

S. Yamasaki
Electrotechnical Laboratory, 1-1-4 Umezono, Tsukuba-City, Ibaraki, 305, Japan

H. Itoh and Y. Morita
Takasaki Radiation Chemistry Establishment, Japan Atomic Energy Research Institute, Takasaki-City, Gunma 370-12, Japan
(Received 6 June 1991)

Electron-paramagnetic-resonance and electron-nuclear-double-resonance (ENDOR) methods are used to identify the negatively charged state of the isolated vacancy in electron-irradiated synthetic diamond crystals. The T_d symmetry is confirmed by determining the arrangement of both nearest neighbors and next-nearest neighbors. ENDOR measurements reveal that the effective spin is $\frac{3}{2}$.

The lattice vacancy is the primary defect that is produced upon irradiation with energetic particles. In diamond, isolated lattice vacancies have been studied mainly by optical measurements following room-temperature irradiation with 1–2-MeV electrons. The GR1 optical-absorption band, which consists of a prominent zero-phonon line at 1.673 eV and phonon-assisted structure at higher energies centered at about 2.0 eV, is assigned to be associated with the neutral vacancy.[1] The ND1 optical-absorption band, which consists of a sharp zero-phonon line at 3.149 eV and phonon-assisted structure at higher energies centered at about 3.4 eV, has been assigned to be associated with the negative vacancy.[2]

In a simple one-electron molecular-orbital model of the nondistorted vacancy, the linear combination of the dangling-bond atomic orbitals (LCAO) of the four atoms around the vacancy forms the defect molecular orbitals: an a_1 singlet and a t_2 triplet. The electronic ground state of the negative vacancy is ${}^4A_2(a_1^2t_2^3)$. The most probable ground states predicted from many-electron LCAO calculations are ${}^2T_2$ ($S=\frac{1}{2}$) for the positively charged vacancy, ${}^1E_1$ ($S=0$) for the neutral vacancy, and ${}^4A_2$ ($S=\frac{3}{2}$) for the negatively charged vacancy.[3–6] The ordering of the lowest electronic levels is sensitive both to the choice of atomic functions used to represent the $2s$ and $2p$ orbitals of carbons and to the extent of the symmetric relaxation. An orbitally nondegenerate, high-spin state ${}^4A_2$ which is not subject to Jahn-Teller distortion appears among the possible ground states only for the negative charge state. Thus, if the isolated vacancy has T_d symmetry and an effective spin $S=\frac{3}{2}$, the charge state is identified to be -1.

In studying vacancies in silicon, the principal experimental tool for the microscopic identification has been electron paramagnetic resonance (EPR).[7] In the negative vacancy in silicon, the symmetry is lowered to C_{2v} resulting in the effective spin $S=\frac{1}{2}$.[8] The EPR spectrum labeled $S1$ ($g=2.0023$) in electron-irradiated type-IIa diamond was ascribed to the positively charged vacancy with an effective spin $S=\frac{1}{2}$.[9,10] The intensity of the $S1$ spectrum was enhanced by illuminating with light $h\nu>2.83$ eV. In this Brief Report, we report that the $S1$ center is the negative vacancy with an effective spin $S=\frac{3}{2}$.

We used crystals in which the negative charge state was a stable form of vacancies produced. While the GR1 center is a dominant product of irradiating relatively pure diamond (type-IIa), the ND1 center occurs in strength when a sufficient concentration of nitrogen is present in the lattice (types-Ia and -Ib).[11] The intensity of the nitrogen signals needs to be low to minimize the disturbance on the EPR and ENDOR measurements of the negative vacancy. Two synthetic diamond crystals, denoted A and B, were grown by the temperature-gradient method using Ni–2 wt. % Ti solvent. The carbon source of sample B was $\sim$10% enriched in ${}^{13}C$ ($I=\frac{1}{2}$, natural abundance 1.1%). After electron irradiation at room temperature (2 MeV, 9.7 h, total fluence 7.8×10^{17} e/cm^2), both crystals showed ND1 as well as

TABLE I. Principal values of ${}^{13}C$ hyperfine tensor (MHz).

T (K)	Nearest neighbors	Next-nearest neighbors	
300	$A_\parallel=141.5$	$A_\parallel=13.3$	Ref. 9
	$A_\perp=81.8$	$A_\perp=9.3$	
77	$A_\parallel=141.5$	$A_\parallel=13.5$	this work
	$A_\perp=81.9$	$A_\perp=9.5$	
4	$A_\parallel=141.8$	$A_1=13.42$	this work
	$A_\perp=81.7$	$A_2=9.40$	
		$A_3=9.23$	

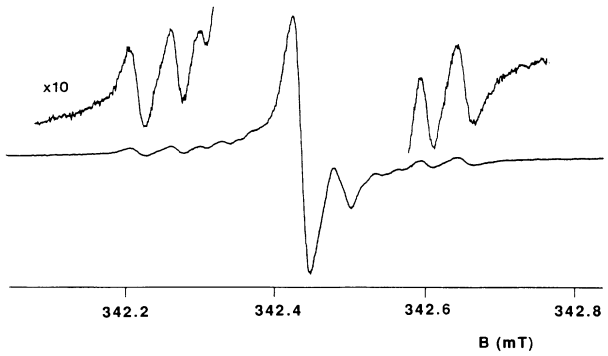

FIG. 1. EPR spectrum of diamond sample A at 4 K showing the ^{13}C hyperfine lines of the next-nearest neighbors ($\mathbf{B}\|$ [110], ν=9.5987 GHz, microwave power 0.5 μW, 100-kHz field modulation).

GR1 optical absorption. The EPR measurements were performed with a Bruker ESP 300 X-band spectrometer. The ENDOR spectra of sample B were taken using a Bruker ESP353 accessory. Since the crystals exhibit a nonuniform color distribution, the impurities (isolated substitutional nitrogen, substitutional Ni^-, interstitial Ni^+) (Refs. 12–14) and vacancies produced are likely to be segregated into different growth sectors of the crystals. The average concentrations obtained from the EPR signal intensities before irradiation were [N] = 0.9 ppm, $[Ni_s^-]$=0.5 ppm, $[Ni_i^+]$=2 ppm for sample A (18.2 mg), and [N] = 8 ppm and $[Ni_s^-]$=3 ppm for sample B (16.6 mg). After irradiation, the average concentrations of the $S1$ center produced were 0.3 and 9 ppm for samples A and B, respectively.

The $S1$ EPR spectrum of sample A has a peak-to-peak linewidth 0.021 mT for the magnetic field $\mathbf{B}$ along [001] and 0.024 mT for $\mathbf{B}$ along [111], allowing observation of both ^{13}C hyperfine lines of nearest neighbors and those of next-nearest neighbors in natural abundance. As the crystal is rotated, the g value (2.0027 at 77 and at 4 K) does not vary to within a relative accuracy of $\pm 0.000\,01$.[15] Both the g value and the ^{13}C hyperfine couplings (Table I) agree with those given in Ref. 9. In the

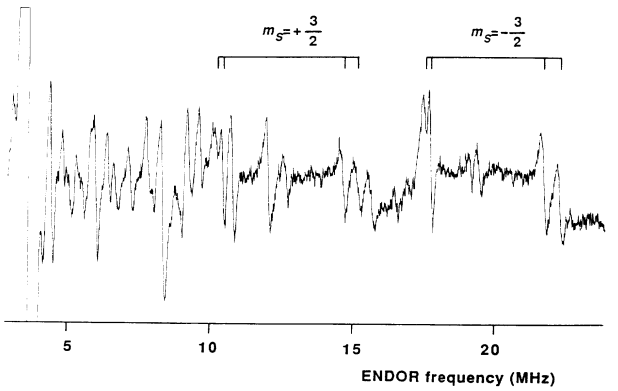

FIG. 2. ENDOR spectrum of diamond sample B (10% ^{13}C) at 4 K showing the next-nearest-neighbor ^{13}C ENDOR lines of the $m_s=\pm\frac{3}{2}$ manifold ($\mathbf{B}\|$ [110], ν=9.4619 GHz, microwave power 0.2 mW, radiofrequency power 68 W).

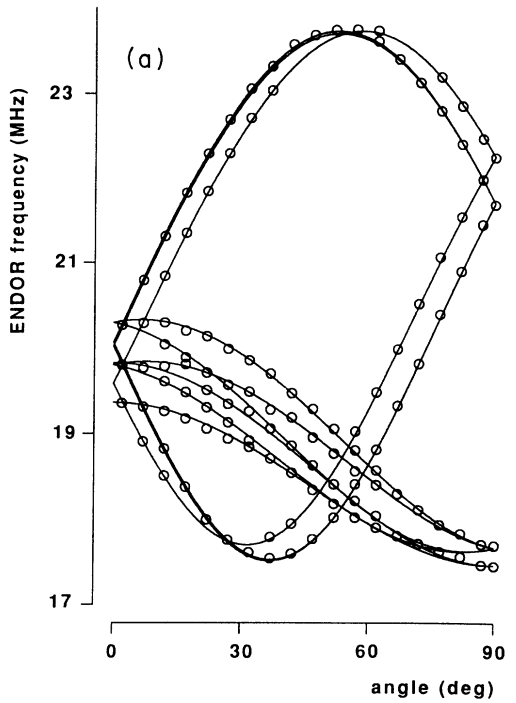

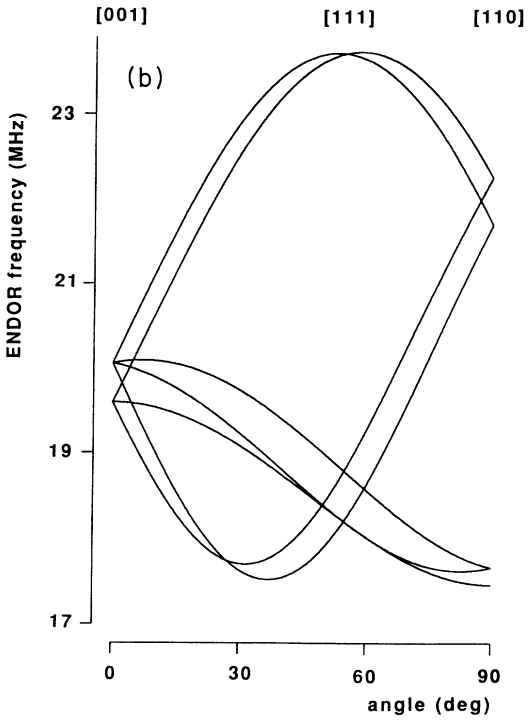

FIG. 3. Angular dependence of the next-nearest-neighbor ^{13}C ENDOR frequencies of the $m_s=-\frac{3}{2}$ manifold for rotation about the [$\bar{1}$10] axis at 4 K. (a) The circles are experimental line positions. Solid lines are calculated by using the hyperfine parameters and the correction of the misalignment of the rotation axis, which are obtained by least-squares fitting. The rotation axis was inclined by 2.3° toward [001] in the (110) plane. (b) Plots calculated for the case without misalignment.

diamond lattice, there are many sets of equivalent carbons around the vacancy. The hyperfine tensors reflect the symmetry properties.[16] If the T_d symmetry is maintained, the four nearest neighbors and the twelve next-nearest neighbors belong to the 111 class and to the 110 class, respectively. By using sample B, it is confirmed that the satellite lines with larger splittings are ^{13}C hyperfine lines of the nearest neighbors (the peak height ratio between the satellite line and the main line is 0.17 for **B** along [001]). Our experiments appear to rule out the model that the satellite lines with larger splittings do not belong to the $S1$ center.[10] The hyperfine tensor of the nearest neighbors is uniaxial around [111]. The isotropy of g and the angular dependence of the ^{13}C hyperfine lines from the nearest neighbors denote the T_d symmetry even at 4 K. EPR spectra of sample A, upon rotation of **B** in the $(\bar{1}10)$ plane, resolved at most only three sets of next-nearest-neighbor hyperfine lines. The resolution of the EPR measurements was not sufficient to determine symmetry class of the next-nearest neighbors. The ^{13}C hyperfine couplings of the next-nearest neighbors (at 300 K in Ref. 9 and at 77 K in our work) were obtained by taking the hyperfine tensor to be uniaxial around the [111] axis. The diamond lattice has two tetrahedral sites (substitutional and interstitial). Vacancies occur at the substitutional site. The next-nearest neighbors of the interstitial sites belong to the 100 class. A definitive assignment of the vacancy retaining the T_d symmetry can be made by confirming that the next-nearest neighbors do belong to the 110 class.

The effective spin of a paramagnetic center having T_d symmetry is difficult to determine using conventional EPR techniques because fine-structure splittings vanish for $S=\frac{1}{2}$, 1, and $\frac{3}{2}$. We determined the spin state of the $S1$ center from the next-nearest neighbor ^{13}C ENDOR frequencies, since they depend on the value of m_s. To first order, the ENDOR frequencies are $h\nu=|m_s A_{\text{eff}}-g_n\mu_n B|$, where A_{eff} are the hyperfine splittings. With **B** along [110], approximate values of A_{eff} measured from the EPR are 0.332 and 0.438 mT at 4 K (Fig. 1). For $S=\frac{3}{2}$, the corresponding ENDOR frequencies at $B=337.20$ mT are estimated to be 10.4 and 14.8 MHz for the $m_s=+\frac{3}{2}$ manifold and 17.6 and 22.0 MHz for the $m_s=-\frac{3}{2}$ manifold, assuming A_{eff} positive and $g_n=1.4044$ The measured ENDOR frequencies of 10.20, 10.45, 14.57, 15.10, 17.46, 17.70, 21.72, and 22.28 MHz at 4 K (Fig. 2) are consistent with this interpretation. Thus, the effective spin of the $S1$ center is $\frac{3}{2}$. With the much higher available resolution of the ENDOR technique, the angular dependence of the ENDOR frequencies shows that the next-nearest neighbors belong to the 110 class (Fig. 3).[17] The principal values of the hyperfine tensor at 4 K were calculated from the angular dependence in Fig. 3 using the first-order equation and are included in Table I. The principal axis with the largest principal value is 120.6° from the [001] axis in the $(\bar{1}10)$ plane. The principal value A_3 is associated with the principal axis along the $[\bar{1}10]$ axis.

With the determination of the spin state $S=\frac{3}{2}$ and the confirmation of the T_d symmetry, the $S1$ center is unambiguously identified to be the negative vacancy. From the uniaxial stress measurements on the zero-phonon line, the ND1 band was assigned to be a transition between an orbitally nondegenerate A ground state and a triply degenerate T excited state at a tetrahedral site.[11] Our EPR measurements support the assignment that the ND1 band arises from the negative vacancy. From the isotropic part A_{iso} and the anisotropic part b of the hyperfine tensors, contributions of the carbon $2s$ and $2p$ orbitals to the wave function of the unpaired electrons are estimated.[13,18] The sum of the spin densities on the four nearest neighbors is estimated to be ~ 1.0. In the next-nearest neighbors, b is mainly due to dipolar interaction between the spin density on the nearest neighbors and the ^{13}C nucleus. The sum of the spin densities on the twelve next-nearest neighbors is estimated to be 0.04. The sp hybrid ratio (6.9) of the nearest neighbors indicates a relatively large symmetric relaxation. In contrast with the fact that the negative vacancy in silicon has C_{2v} symmetry with an effective spin $\frac{1}{2}$, the negative vacancy in diamond retains T_d symmetry. Similarly, the symmetry of substitutional Ni^- (Ni_s^-) is different between diamond and silicon. In diamond, Ni_s^- has T_d symmetry with an effective spin $S=\frac{3}{2}$.[13] In silicon, Ni_s^- with an orthorhombic distortion shows $S=\frac{1}{2}$ spectra.[19] When impurities or vacancies are incorporated, lattice distortion should be required to attain the energy minimum configuration. In diamond, which has strong covalent bonding, such a distortion that involves a bending of the bond angles might be less likely to occur than one that involves a radial movement of atoms.[20] It has been reported that the neutral vacancy in GaP which is isoelectronic with the negative vacancy in diamond has T_d symmetry with an effective spin $\frac{3}{2}$.[21,22] While the ground state of vacancies in silicon is adequately described by a single-electron picture, it is suggested that many-electron effects are dominant in determining the electronic properties of intrinsic defects in some semiconductors of relatively wide energy gap.[21] Comparing the negative vacancy in silicon,[23] the neutral vacancy in GaP,[24] and the negative vacancy in diamond, we note a tendency for the electron to be less delocalized beyond the nearest neighbors with an increase in the energy gap.

In summary, EPR and ENDOR measurements reveal that the negative vacancy in diamond has T_d symmetry with an effective spin $\frac{3}{2}$. This confirms the $^4A_2$ ground state predicted by Coulson and Larkins.[6]

[1]See, J. Walker, Rep. Prog. Phys. **42**, 1605 (1978), and references therein.

[2]G. Davies, Nature **269**, 498 (1977).

[3]C. A. Coulson and M. J. Kearsley, Proc. R. Soc. A **241**, 433 (1957).

[4]T. Yamaguchi, J. Phys. Soc. Jpn. **17**, 1359 (1962).

[5]J. Friedel, M. Lannoo, and G. Leman, Phys. Rev. **164**, 1056 (1967).

[6]C. A. Coulson and F. P. Larkins, J. Phys. Chem. Solids **32**, 2245 (1971).

[7]For a recent review, see G. D. Watkins, in *Deep Centers in Semiconductors,* edited by S. T. Pantelides (Gordon and Breach, New York, 1986), pp. 147–183.

[8]G. D. Watkins, in *Radiation Damage in Semiconductors,* edited by P. Baruch (Dunod, Paris, 1965), pp. 97–113.

[9]The $S1$ center was originally labeled A center. See J. A. Baldwin, Jr., Phys. Rev. Lett. **10**, 220 (1963).

[10]J. H. N. Loubser and J. A. van Wyk, Rep. Prog. Phys. **41**, 1201 (1978).

[11]G. Davies and E. C. Lightowlers, J. Phys. C **3**, 638 (1970).

[12]W. V. Smith, P. P. Solokin, I. L. Gelles, and G. J. Lasher, Phys. Rev. **115**, 1546 (1959).

[13]J. Isoya, H. Kanda, J. R. Norris, J. Tang, and M. K. Bowman, Phys. Rev. B **41**, 3905 (1990).

[14]J. Isoya, H. Kanda, and Y. Uchida, Phys. Rev. B **42**, 9843 (1990).

[15]The precision of the g value, in our case, was limited by the uncertainty in the magnetic-field strength which was calibrated by using α,α'-diphenyl-β-picryl hydrazyl ($g=2.0036$).

[16]G. W. Ludwig, Phys. Rev. **137**, A1520 (1965).

[17]The symmetry class of a set of surrounding carbons is assigned from the rotation pattern of the ENDOR line positions. See D. A. van Wezep, R. van Kemp, E. G. Sieverts, and C. A. J. Ammerlaan, Phys. Rev. B **32**, 7129 (1985).

[18]The unpaired electron localized 100% in a carbon $2s$ orbital produces an isotropic hyperfine interaction $a_0=3136$ MHz and in a carbon $2p$ orbital an anisotropic hyprefine interaction $b_0=89.4$ MHz. See B. A. Goodman and J. B. Raynor, in *Advances in Inorganic and Radiochemistry,* edited by H. J. Emeleus and A. G. Sharpe (Academic, New York, 1970), Vol. 13, pp. 135–362.

[19]L. S. Vlasenko, N. T. Són, A. B. van Oosten, C. A. J. Ammerlaan, A. A. Lebedev, E. S. Taptygov, and V. A. Khramtsov, Solid State Commun. **73**, 393 (1990).

[20]G. D. Davies, Rep. Prog. Phys. **44**, 787 (1981).

[21]T. A. Kennedy, N. D. Wilsey, J. J. Krebs, and G. H. Stauss, Phys. Rev. Lett. **50**, 1281 (1983).

[22]J. Hage, J. R. Niklas, and J. -M. Spaeth, Mater. Sci. Forum **10 - 12**, 259 (1986).

[23]M. Sprenger, S. H. Muller, E. G. Sieverts, and C. A. J. Ammerlaan, Phys. Rev. B **35**, 1566 (1987).

[24]T. A. Kennedy and N. D. Wilsey, Phys. Rev. Lett. **41**, 977 (1978).